

# Exact calculations of a quasi-bound state in the $\bar{K}\bar{K}N$ system

N.V. Shevchenko<sup>a1</sup> and J. Haidenbauer<sup>2</sup>

<sup>1</sup>*Nuclear Physics Institute, 25068 Řež, Czech Republic*

<sup>2</sup>*Institute for Advanced Simulation and Jülich Center for Hadron Physics,  
Forschungszentrum Jülich, D-52425 Jülich, Germany*

(Dated: August 3, 2015)

## Abstract

Dynamically exact calculations of a quasi-bound state in the  $\bar{K}\bar{K}N$  three-body system are performed using Faddeev-type AGS equations. As input two phenomenological and one chirally motivated  $\bar{K}N$  potentials are used, which describe the experimental information on the  $\bar{K}N$  system equally well and produce either a one- or two-pole structure of the  $\Lambda(1405)$  resonance. For the  $\bar{K}\bar{K}$  interaction separable potentials are employed that are fitted to phase shifts obtained from two theoretical models. The first one is a phenomenological  $\bar{K}\bar{K}$  potential based on meson exchange, which is derived by SU(3) symmetry arguments from the Jülich  $\pi\pi - \bar{K}K$  coupled-channels model. The other interaction is a variant of the first one, which is adjusted to the  $KK$  s-wave scattering length recently determined in lattice QCD simulations. The position and width of the  $\bar{K}\bar{K}N$  quasi-bound state is evaluated in two ways: (i) by a direct pole search in the complex energy plane and (ii) using an "inverse determinant" method, where one needs to calculate the determinant of the AGS system of equations only for real energies. A quasi-bound state is found with binding energy  $B_{\bar{K}\bar{K}N} = 12 - 26$  MeV and width  $\Gamma_{\bar{K}\bar{K}N} = 61 - 102$  MeV, which could correspond to the experimentally observed  $\Xi(1950)$  state.

PACS numbers: 21.45.+v, 11.80.Jy, 13.75.Lz

---

<sup>a</sup> Corresponding author: shevchenko@ujf.cas.cz

## I. INTRODUCTION

It is generally accepted that the  $\bar{K}N$  interaction in the isospin-zero state is strongly attractive and produces a quasi-bound state, which shows itself as the  $\Lambda(1405)$  resonance in the lower  $\pi\Sigma$  channel. This fact led to the conjecture that a quasi-bound state could also exist in the  $\bar{K}NN$  three-body system. The first paper on the topic appeared more than 50 years ago [1], but it was Ref. [2] which aroused a large interest in the question of the existence and properties of such a state. It triggered many theoretical papers devoted to the  $K^-pp$  system and in the sequel also experimental efforts. However, so far the experimental results neither agree with theoretical predictions nor between themselves. Indeed, the only point on which all theorists agree, is that a quasi-bound state in the  $K^-pp$  really exists. But the actual predictions for its binding energy and width vary over a fairly wide range.

A study with the aim to find a similar quasi-bound state in the  $K^-d$  system, which differs from the  $K^-pp$  by quantum numbers ( $J^P = 1^-$  versus  $0^-$ ) gave negative results [3].

Another possible candidate for a three-body system with a quasi-bound state is  $\bar{K}\bar{K}N$ . In contrast to  $\bar{K}NN$ , however, it contains the  $\bar{K}\bar{K}$  interaction, which is expected to be repulsive [4, 5]. Thus, the principal question is whether the repulsion is strong enough to exclude the possibility of a quasi-bound state formation in the system. A first exploratory investigation of the  $\bar{K}\bar{K}N$  system was presented in Ref. [6]. In this variational calculation based on a simplified two-body input indeed a bound state was found.

In the present paper we report on the first dynamically exact calculation of a quasi-bound state in the  $\bar{K}\bar{K}N$  system. We solve the Faddeev-type Alt-Grassberger-Sandhas (AGS) equations with two phenomenological and one chirally motivated  $\bar{K}N$  potentials. The potentials describe experimental data equally well and produce a one- or two-pole structure of the  $\Lambda(1405)$  resonance. They were originally designed to address the influence of the number of poles of the resonance on various properties of the  $\bar{K}N$  and  $\bar{K}NN$  systems (quasi-bound states in  $K^-pp$  and  $K^-d$ ,  $K^-d$  scattering and  $1s$  level shift and width of kaonic deuterium), an issue which was of relevance for the strangeness physics community, see e.g. [7–9].

There is no experimental information on the  $\bar{K}\bar{K}$  system. However, recently lattice QCD calculations of the  $KK$   $s$ -wave scattering length have become available [10, 11] and we take those results as guideline for constructing the  $\bar{K}\bar{K}$  potential. The published scattering

lengths are small and negative and, thus, suggest a weakly repulsive interaction. On the phenomenological level one can exploit the fact that the  $\bar{K}\bar{K}$  (or  $KK$ ) interaction is related to the one in the  $\bar{K}K$  system via SU(3) flavor symmetry. For the latter several potential models can be found in the literature. We adopt here the  $\pi\pi - \bar{K}K$  coupled channels model developed by the Jülich group [12, 13] as starting point for generating another  $\bar{K}\bar{K}$  interaction. This model, derived in the meson-exchange framework, predicts a somewhat more repulsive  $\bar{K}\bar{K}$  interaction. In the actual calculation separable representations are employed, and we construct the  $\bar{K}\bar{K}$  potentials in such away that they reproduce the phase shifts of the Jülich  $\bar{K}\bar{K}$  meson exchange model and the scattering length of the lattice QCD calculation [11], respectively.

The position and width of the  $\bar{K}\bar{K}N$  quasi-bound state is evaluated in two different ways. First, we perform a direct search for the three-body pole in the complex energy plane. To do this we find the solvability condition of the homogeneous AGS equations. In addition we employ the "inverse determinant" method proposed and successfully used in Ref. [14] for the  $K^-pp$  system. It consists in the calculation of the inverse determinant of the kernel of the AGS equations and fitting a Breit-Wigner type function to the peak in its modulus squared.

The paper is structured in the following way: The three-body equations, which were derived and solved, are described in the next section. The two-body interactions, being an input for the AGS equations, can be found in Section III. The obtained results are presented and discussed in the Section IV, while the last section contains our conclusions.

## II. AGS EQUATIONS

The  $\bar{K}N$  system is coupled to other channels, in particular, to the  $\pi\Sigma$  system, where the  $\Lambda(1405)$  resonance is observed. Since it was shown in [15] that a proper inclusion of the  $\pi\Sigma$  channel is important for the  $\bar{K}NN$  system, we assume that the same is also the case for  $\bar{K}\bar{K}N$ . The three-body Faddeev-type AGS equations for the  $\bar{K}\bar{K}N$  system with coupled  $\bar{K}\pi\Sigma$  channel are of the form

$$U_{ij}^{\alpha\beta} = (1 - \delta_{ij})\delta_{\alpha\beta}(G_0^\alpha)^{-1} + \sum_{k=1}^3 \sum_{\gamma=1}^3 (1 - \delta_{ik}) T_k^{\alpha\gamma} G_0^\gamma U_{kj}^{\gamma\beta}, \quad (1)$$

where the unknown operators  $U_{ij}^{\alpha\beta}$  describe the elastic and re-arrangement processes  $j^\beta + (k^\beta i^\beta) \rightarrow i^\alpha + (j^\alpha k^\alpha)$ . The operator  $G_0^\alpha$  in Eq. (1), which is diagonal in the 'particle' indices, is the free three-body Green's function. The Faddeev partition indices  $i, j = 1, 2, 3$  denote simultaneously an interacting pair and a spectator particle, while the 'particle' indices  $\alpha, \beta = 1, 2, 3$  denote the three-body channels. The partition and 'particle' channel indices denoting the two-body subsystems are summarized in Table I.

TABLE I. Partition ( $i$ ) and 'particle' channel ( $\alpha$ ) indices of the operators in the AGS system of equations (1) denoting the two-body subsystems. The interactions are further labelled by the two-body isospin values, entering the system before symmetrisation.

$i \setminus \alpha$	1 ( $\bar{K}\bar{K}N$ )	2 ( $\bar{K}\pi\Sigma$ )	3 ( $\pi\bar{K}\Sigma$ )
1	$\bar{K}N_{I=0,1}$	$\pi\Sigma_{I=0,1}$	$\bar{K}\Sigma_{I=\frac{1}{2},\frac{3}{2}}$
2	$\bar{K}N_{I=0,1}$	$\bar{K}\Sigma_{I=\frac{1}{2},\frac{3}{2}}$	$\pi\Sigma_{I=0,1}$
3	$\bar{K}\bar{K}_{I=0,1}$	$\bar{K}\pi_{I=\frac{1}{2},\frac{3}{2}}$	$\bar{K}\pi_{I=\frac{1}{2},\frac{3}{2}}$

The operators  $T_i^{\alpha\beta}$  in Eq. (1) are two-body  $T$ -matrices immersed into the three-body space. For the description of the two-body interactions we use separable potentials

$$V_{i,I}^{\alpha\beta} = \lambda_{i,I}^{\alpha\beta} |g_{i,I}^\alpha\rangle\langle g_{i,I}^\beta|, \quad (2)$$

which depend on the two-body isospin  $I$  and lead to a separable form of the corresponding  $T$ -matrices:

$$T_{i,I}^{\alpha\beta} = |g_{i,I}^\alpha\rangle\tau_{i,I}^{\alpha\beta}\langle g_{i,I}^\beta|. \quad (3)$$

Separable potentials allow one to introduce new transition and kernel operators defined via

$$X_{ij,I_i I_j}^{\alpha\beta} = \langle g_{i,I_i}^\alpha | G_0^\alpha U_{ij,I_i I_j}^{\alpha\beta} G_0^\beta | g_{j,I_j}^\beta \rangle, \quad (4)$$

$$Z_{ij,I_i I_j}^{\alpha\beta} = \delta_{\alpha\beta} Z_{ij,I_i I_j}^\alpha = \delta_{\alpha\beta} (1 - \delta_{ij}) \langle g_{i,I_i}^\alpha | G_0^\alpha | g_{j,I_j}^\alpha \rangle, \quad (5)$$

to obtain a simpler system of equations than that in Eq. (1):

$$X_{ij,I_i I_j}^{\alpha\beta} = \delta_{\alpha\beta} Z_{ij,I_i I_j}^\alpha + \sum_{k=1}^3 \sum_{\gamma=1}^3 \sum_{I_k} Z_{ik,I_i I_k}^\alpha \tau_{k,I_k}^{\alpha\gamma} X_{kj,I_k I_j}^{\gamma\beta}. \quad (6)$$

The free three-body Hamiltonian of the channel  $\alpha$  is defined in momentum representation by

$$H_0^\alpha = \frac{(k_i^\alpha)^2}{2m_{jk}^\alpha} + \frac{(p_i^\alpha)^2}{2\mu_i^\alpha}, \quad (7)$$

where  $m_{jk}^\alpha$  and  $\mu_i^\alpha$  are two- and three-body reduced masses, respectively

$$m_{jk}^\alpha = \frac{m_j^\alpha m_k^\alpha}{m_j^\alpha + m_k^\alpha}, \quad \mu_i^\alpha = \frac{m_i^\alpha(m_j^\alpha + m_k^\alpha)}{m_i^\alpha + m_j^\alpha + m_k^\alpha}, \quad i \neq j \neq k. \quad (8)$$

Three Jacobi momentum coordinate sets  $|\vec{k}_i^\alpha, \vec{p}_i^\alpha\rangle$ ,  $i = 1, 2, 3$ ,  $\alpha = 1, 2, 3$  are used, where  $\vec{k}_i^\alpha$  is the center-of-mass momentum of the  $(jk)$  pair and  $\vec{p}_i^\alpha$  is the momentum of the spectator  $i$  with respect to the pair  $(jk)$ ,  $i \neq j \neq k$ .

In momentum representation the operators  $X$  and  $Z$  are integrated over the Jacobi momenta  $\vec{k}_i^\alpha$ . Therefore, the operators act on the second momentum,  $\vec{p}_i^\alpha$

$$\langle \vec{p}_i^\alpha | X_{ij, I_i I_j}^{\alpha\beta}(z_{tot}) | \vec{p}_j'^\beta \rangle = X_{ij, I_i I_j}^{\alpha\beta}(\vec{p}_i^\alpha, \vec{p}_j'^\beta; z_{kin}^\alpha + z_{th}^\alpha), \quad (9)$$

$$\langle \vec{p}_i^\alpha | Z_{ij, I_i I_j}^\alpha(z_{tot}) | \vec{p}_j'^\alpha \rangle = Z_{ij, I_i I_j}^\alpha(\vec{p}_i^\alpha, \vec{p}_j'^\alpha; z_{kin}^\alpha + z_{th}^\alpha), \quad (10)$$

where the total energy  $z_{tot} = z_{th}^\alpha + z_{kin}^\alpha$  is the sum of the channel kinetic energy  $z_{kin}^\alpha$  and the channel threshold energy  $z_{th}^\alpha = \sum_{i=1}^3 m_i^\alpha$ . The energy-dependent part of a two-body  $T$ -matrix, embedded in the three-body space, is defined by the following relation:

$$\langle \vec{p}_i^\alpha | \tau_{i, I_i}^{\alpha\beta}(z_{tot}) | \vec{p}_j'^\beta \rangle \equiv \delta_{ij} \delta(\vec{p}_i^\alpha - \vec{p}_j'^\beta) \tau_{i, I_i}^{\alpha\beta} \left( z_{tot} - z_{th}^\alpha - \frac{(p_i^\alpha)^2}{2\mu_i} \right). \quad (11)$$

Since the antikaon is a pseudoscalar meson, the total spin of the  $\bar{K}\bar{K}N$  system is equal to one half. All our two-body interactions have zero orbital angular momentum, therefore, the total angular momentum  $J$  is also 1/2. As for the isospin, we consider the three-body system with the lowest possible value, i.e. with  $I^{(3)} = 1/2$ .

In what follows the indices on the right-hand side of the operators  $X_{ij, I_i I_j}^{\alpha\beta}$  will be omitted, i.e.  $X_{ij, I_i I_j}^{\alpha\beta} \rightarrow X_{i, I_i}^\alpha$ , since they denote the initial state, which is fixed for a given system. To search for a quasi-bound state means to look for a solution of the homogeneous equations

$$X_{i, I_i}^\alpha = \sum_{k=1}^3 \sum_{\gamma=1}^3 \sum_{I_k} Z_{ik, I_i I_k}^\alpha \tau_{k, I_k}^{\alpha\gamma} X_{k, I_k}^\gamma, \quad (12)$$

which however, should be symmetrized first since there are two identical mesons in the  $\bar{K}\bar{K}N$  system. The  $X_{3,1}^1$  transition operator has the proper symmetry properties already

(while  $X_{3,0}^1$  is antisymmetric). The remaining operators acquire the necessary symmetry properties in the following combinations:

$$\begin{aligned}
X_{1,0}^{1,sm} &= X_{1,0}^1 + X_{2,0}^1, & X_{1,1}^{1,sm} &= X_{1,1}^1 + X_{2,1}^1, \\
X_{1,0}^{2,sm} &= X_{1,0}^2 + X_{2,0}^3, & X_{1,1}^{2,sm} &= X_{1,1}^2 + X_{2,1}^3, \\
X_{2,\frac{1}{2}}^{2,sm} &= X_{2,\frac{1}{2}}^2 + X_{1,\frac{1}{2}}^3, & X_{2,\frac{3}{2}}^{2,sm} &= X_{2,\frac{3}{2}}^2 + X_{1,\frac{3}{2}}^3, \\
X_{3,\frac{1}{2}}^{2,sm} &= X_{3,\frac{1}{2}}^2 - X_{3,\frac{1}{2}}^3, & X_{3,\frac{3}{2}}^{2,sm} &= X_{3,\frac{3}{2}}^2 + X_{3,\frac{3}{2}}^3.
\end{aligned} \tag{13}$$

In momentum representation the system of operator equations (12) turns into a system of integral equations, schematically given by

$$X_i(p) = \int_0^\infty Z_{ij}(p, p'; z) \tau_j \left( z - \frac{p'^2}{2\mu_j} \right) X_j(p') dp'. \tag{14}$$

This system is then discretized, and the value of  $z$  at which the determinant of the kernel matrix  $A_{mn}(z) = [Z(z) \tau(z)]_{mn}$  is equal to zero is determined. This complex energy, located on the proper energy sheet, corresponds to the pole of the quasi-bound state.

In the present study we determine the pole position in two ways. First, we perform a direct search of the pole in the complex energy plane as described above. For that purpose we have to rotate the contour of the integration in Eq. (14) into the complex momentum plane in order to avoid irregular regions and singularities, see Ref. [14] for a detailed discussion.

Since the analytic continuation of the integral equations into the complex plane is a non-trivial procedure, we employ here in addition the inverse determinant method proposed and successfully applied in Ref. [14] for the  $K^-pp$  system. It uses the fact that the function  $1/|Det A(z)|^2$ , calculated along the real energy axis  $z$ , exhibits a resonance shape in the neighbourhood of the pole position. This bump can be fitted using the Breit-Wigner type formula, and the position and the width of the resonance can be estimated. Since the calculations in this case are performed on the real energy axis, it allows to avoid possible problems with the analytic continuation of the equations into the complex momentum plane.

It was demonstrated in Ref. [14] that the two methods are indeed complementary. However, it is necessary to keep in mind that the second method gives a reliable estimation of the pole position only in the case where the resonance is quite narrow and, therefore, the produced bump is fairly pronounced.

### III. INTERACTIONS

The explicit form of the one-term separable potentials, introduced in Eq. (2), in momentum representation is

$$V_{i,I_i}^{\alpha\beta}(k_i^\alpha, k_i'^\beta) = \lambda_{i,I_i}^{\alpha\beta} g(k_i^\alpha) g(k_i'^\beta). \quad (15)$$

The used  $\bar{K}N$  and  $\bar{K}\bar{K}$  interactions are described in the following subsections. The remaining interactions in the three-body system with coupled  $\bar{K}\bar{K}N$  and  $\bar{K}\pi\Sigma$  channels are those in the lower-lying three-body channel, namely  $\pi\Sigma$ ,  $\bar{K}\Sigma$ , and  $\bar{K}\pi$ . The first one,  $\pi\Sigma$ , is part of the employed coupled-channel model for the  $\bar{K}N$  interaction. Almost nothing is known about the  $\bar{K}\Sigma$  interaction, in particular, there is no experimental information. There are suggestions [16, 17] that this strangeness  $S = -2$  system can form and couple to  $\Xi$  resonances. The  $\bar{K}\pi$  system is related to  $K\pi$  via charge conjugation and for the latter phase shifts are available [18–20]. Thus, in principle, it would be possible to construct a potential in a similar way as for the  $\bar{K}N$  interaction described below by fitting its parameters to those phase shifts. However, we assume that these two interactions in the lower three-body channel are not so important for the system under consideration and can be omitted. In any case, keeping in mind the unclear situation with regard to the  $\bar{K}\Sigma$  interaction, an inclusion of those channels into the calculation would not lead to quantitatively better constrained  $\bar{K}\bar{K}N$  quasi-bound state results.

Therefore, our three-body calculation with the coupled  $\bar{K}\bar{K}N - \bar{K}\pi\Sigma$  channels has only one non-zero interaction in the lower channel: the  $\pi\Sigma$ , coupled to the  $\bar{K}N$ . Then our two-channel three-body calculation with coupled-channel  $\bar{K}N - \pi\Sigma$  potential is equivalent to the one-channel three-body calculation utilizing the so-called exact optical  $\bar{K}N$  potential, see [21]. We performed calculations based on both formulations and obtained perfect agreement between their results.

#### A. Antikaon-nucleon interaction

Several models of the  $\bar{K}N$  interaction were constructed by us in the past for application in our works devoted to the  $\bar{K}NN$  system. In the present study we employ three of those. In particular, we use the two phenomenological  $\bar{K}N - \pi\Sigma$  potentials that yield a one- or two-pole structure of the  $\Lambda(1405)$  resonance which were presented in [22]. The form factors

of the one-pole version of the potential and those of the  $\bar{K}N$  channel of the two-pole version have a Yamaguchi form

$$g_I^\alpha = \frac{1}{(k^\alpha)^2 + (\beta_I^\alpha)^2}, \quad (16)$$

while a slightly more complicated form is used for the  $\pi\Sigma$  channel

$$g_I^\alpha = \frac{1}{(k^\alpha)^2 + (\beta_I^\alpha)^2} + \frac{s(\beta_I^\alpha)^2}{[(k^\alpha)^2 + (\beta_I^\alpha)^2]^2} \quad (17)$$

in the two-pole model of the interaction.

Recently, a chirally motivated potential describing the coupled  $\bar{K}N - \pi\Sigma - \pi\Lambda$  channels was constructed and used in [3]. In contrast to the energy independent phenomenological models mentioned above the chirally motivated potential has strength constants  $\lambda_{i,I_i}^{\alpha\beta}(z^{(2)})$ , which depend on the energy in the two-body subsystem  $z^{(2)}$ .

All three potentials were fitted to data on  $\bar{K}N$  scattering and characteristics of kaonic hydrogen. In particular, the potentials reproduce the measured cross sections of elastic ( $K^-p \rightarrow K^-p$ ) and inelastic ( $K^-p \rightarrow \bar{K}^0n$ ,  $K^-p \rightarrow \pi^+\Sigma^-$ ,  $K^-p \rightarrow \pi^-\Sigma^+$ ,  $K^-p \rightarrow \pi^0\Sigma^0$ ,  $K^-p \rightarrow \pi^0\Lambda$ ) scattering (the last reaction is described by the chirally motivated potential only) from different experiments [23–27].

They also reproduce the accurately measured threshold branching ratios  $\gamma$ ,  $R_c$  and  $R_n$  [28, 29]

$$\gamma = \frac{\Gamma(K^-p \rightarrow \pi^+\Sigma^-)}{\Gamma(K^-p \rightarrow \pi^-\Sigma^+)} = 2.36 \pm 0.04 \quad (18)$$

$$R_c = \frac{\Gamma(K^-p \rightarrow \pi^+\Sigma^-, \pi^-\Sigma^+)}{\Gamma(K^-p \rightarrow \text{all inelastic channels})} = 0.664 \pm 0.011, \quad (19)$$

$$R_n = \frac{\Gamma(K^-p \rightarrow \pi^0\Lambda)}{\Gamma(K^-p \rightarrow \text{neutral states})} = 0.189 \pm 0.015. \quad (20)$$

Since the  $\pi\Lambda$  channel is taken into account in the phenomenological potentials indirectly, through an imaginary part of one of the  $\lambda^{\alpha\beta}$  parameters, we constructed a new threshold branching ratio based on  $R_c$  and  $R_n$ :

$$R_{\pi\Sigma} = \frac{\Gamma(K^-p \rightarrow \pi^+\Sigma^-) + \Gamma(K^-p \rightarrow \pi^-\Sigma^+)}{\Gamma(K^-p \rightarrow \pi^+\Sigma^-) + \Gamma(K^-p \rightarrow \pi^-\Sigma^+) + \Gamma(K^-p \rightarrow \pi^0\Sigma^0)}, \quad (21)$$

which has an “experimental” value (derived from the experimental data on  $R_c$  and  $R_n$ )

$$R_{\pi\Sigma} = \frac{R_c}{1 - R_n(1 - R_c)} = 0.709 \pm 0.011. \quad (22)$$

The chirally motivated potential reproduces all three experimental branching ratios directly.

Finally, all three  $\bar{K}N$  models reproduce the most recent experimental results of the SIDDHARTA experiment [30] on the  $1s$  level shift  $\Delta E_{1s}$  and width  $\Gamma_{1s}$  of kaonic hydrogen

$$\Delta E_{1s} = -283 \pm 36 \pm 6 \text{ eV}, \quad \Gamma_{1s} = 541 \pm 89 \pm 22 \text{ eV}. \quad (23)$$

Note that those quantities were calculated directly, without using some approximate formula. All  $\bar{K}N$  results were obtained by solving coupled-channels Lippmann-Schwinger equation with the strong interaction plus the Coulomb potential. In addition, the physical masses of the involved particles were used, so that the associated two-body isospin nonconservation is properly included. However, the three-body calculations are performed with isospin averaged masses and without Coulomb interaction for simplicity reasons but also because we expect the pertinent effects to be small.

Irrespective of the number of poles that constitute the  $\Lambda(1405)$  resonance, which appears as a quasi-bound state in the  $\bar{K}N$  channel and as a resonance in the lower channels, for all considered potentials the resulting isospin-zero elastic  $\pi\Sigma$  cross sections has a peak near the position of the resonance as given by the Particle Data Group (PDG) with comparable width ( $M_{\Lambda(1405)} = 1405.1 \text{ MeV}$ ,  $\Gamma_{\Lambda(1405)} = 50.5 \text{ MeV}$  according to the most recent issue [31]).

All three  $\bar{K}N$  potentials describe the experimental information with the same level of accuracy, as one can see in Refs. [22] and [3] for the phenomenological and chirally motivated potentials, respectively. The actual parameters of the potentials can be found in those papers.

## B. Antikaon-antikaon interaction

There is no experimental information on the  $\bar{K}\bar{K}$  interaction and, therefore, the  $\bar{K}\bar{K}$  potential cannot be constructed in the same way as the one for  $\bar{K}N$ . Hence, we resort to theory and adopt here the  $\pi\pi - \bar{K}K$  coupled channels model developed by the Jülich group [12, 13] some time ago as guideline. Indeed, based on the underlying SU(3) flavor symmetry the interaction in the  $\bar{K}\bar{K}$  system (or equivalently in the  $KK$  system) can be directly deduced from the  $\bar{K}K$  interaction of Ref. [13] without any further assumptions. A detailed description of the Jülich  $\pi\pi - \bar{K}K$  meson exchange model can be found in Refs. [12, 13]. Here we provide only a short summary of the interaction.

The dynamical input that constitutes the Jülich  $\pi\pi - \bar{K}K$  model is depicted in Fig. 1.

The figure contains only  $s$ - and  $t$ -channel diagrams;  $u$ -channel processes corresponding to the considered  $t$ -channel processes are also included whenever they contribute. The scalar-isoscalar particle denoted by  $f_0$  in Fig. 1 (and  $\epsilon$  in Ref. [13]) effectively includes the singlet and the octet member of the scalar nonet. The effects of  $t$ -channel  $f_2(1270)$  and  $f_0$  exchange were found to be negligible [13] and, therefore, not included in the model.

The coupling constant  $g_{\rho\pi\pi}$ , required for  $t$ - and  $u$ -channel exchange diagrams, is determined from the decay widths of the  $\rho$ . Most of the other coupling constants are determined from SU(3) symmetry relations, and standard assumptions about the octet/singlet mixing angles, as described in Ref. [12]. The Jülich  $\pi\pi - \bar{K}K$  potential contains also vertex form factors and those are parametrized in the conventional monopole or dipole form, cf. the Appendix of Ref. [13]. The values of the inherent cutoff masses have been determined in a fit to the  $\pi\pi$  phase shifts.

This interaction yields a good description of the  $\pi\pi$  phase shifts up to partial waves with total angular momentum  $J = 2$  and for energies up to  $z_{\pi\pi} \approx 1.4$  GeV as can be seen in Ref. [13]. Furthermore, as a special feature, the  $f_0(980)$  meson results as a dynamically generated state, namely as a quasi-bound  $\bar{K}K$  state. Also the  $a_0(980)$  is found to be dynamically generated in the corresponding  $\pi\eta - \bar{K}K$  system.

The interaction in the  $\bar{K}\bar{K}$  (or the  $KK$ ) system follows directly from the one for  $\bar{K}K$  by invoking SU(3) symmetry arguments. It is provided by vector-meson exchange ( $\rho$ ,  $\omega$ ,  $\phi$ ) with coupling constants fixed according to standard SU(3) relations, see Table I of [13]. For identical particles the Bose-Einstein statistics applies and it restricts the  $\bar{K}\bar{K}$   $s$ -wave to be solely in isospin  $I = 1$ . In this case the contributions of the three vector-meson exchanges add up coherently and they are all repulsive so that one expects an overall repulsive interaction in the  $\bar{K}\bar{K}$   $s$ -wave. Indeed the  $\bar{K}\bar{K}$  scattering length predicted by the Jülich model is  $a_{\bar{K}\bar{K}, I=1} = -0.186$  fm. This version of the  $\bar{K}\bar{K}$  interaction will be called 'Original'.

Recently, results for the  $KK$  scattering length have become available from lattice QCD simulations [10, 11]. Those calculations, performed for quark masses corresponding to  $m_\pi = 170 - 710$  MeV, suggest values of  $a_{\bar{K}\bar{K}, I=1} = (-0.141 \pm 0.006)$  fm [11] and  $a_{\bar{K}\bar{K}, I=1} = (-0.124 \pm 0.006 \pm 0.013)$  fm [10], respectively, when extrapolated to the physical point. Since those values are noticeably smaller than the one predicted by the Jülich meson-exchange model and, accordingly, imply a somewhat less repulsive  $\bar{K}\bar{K}$  interaction we construct also an interaction that is in line with the lattice QCD results. A corresponding potential can

be easily generated by simply reducing the values of the cutoff masses for the vector-meson exchange in the Jülich model until the scattering length suggested by the lattice QCD calculations is reproduced. The interaction constructed with that aim yields  $a_{\bar{K}\bar{K},I=1} = -0.142$  fm, close to the result by the NPLQCD collaboration [11]. This version of the  $\bar{K}\bar{K}$  interaction will be called 'Lattice motivated'.

We cannot use the models of the  $\bar{K}\bar{K}$  interaction described above directly in the AGS equations. Therefore, we represent also the  $\bar{K}\bar{K}$  interaction in form of one-term separable potentials, see Eq. (15), with form factors given by

$$g(k) = \frac{1}{\beta_1^2 + k^2} + \frac{\gamma}{\beta_2^2 + k^2}. \quad (24)$$

The strength parameters  $\lambda$ ,  $\gamma$  and range parameters  $\beta$  are fixed by a fit to the  $\bar{K}\bar{K}$  phase shifts and scattering lengths of the 'Original' Jülich model and the 'Lattice motivated' interaction. The phase shifts predicted by the initial interactions and those of the corresponding separable potentials are displayed in Fig. 2, so that one can see the quality of the reproduction.

#### IV. RESULTS AND DISCUSSION

The results of our calculations are summarized in Table II for various combinations of the employed  $\bar{K}\bar{K}$  and  $\bar{K}N$  interactions. We used the two  $\bar{K}\bar{K}$  interactions (Original  $V_{\bar{K}\bar{K}}^{Orig}$  and Lattice-motivated  $V_{\bar{K}\bar{K}}^{Latt}$ ) described in the Section III B and three  $\bar{K}N$  potentials, namely the phenomenological one-pole  $V_{\bar{K}N-\pi\Sigma}^{1,SIDD}$  and two-pole  $V_{\bar{K}N-\pi\Sigma}^{2,SIDD}$  potentials from [22], and the chirally-motivated  $V_{\bar{K}N-\pi\Sigma-\pi\Lambda}^{Chiral}$  from [3] discussed in Section III A. The pole positions of the quasi-bound state in the  $\bar{K}\bar{K}N$  system were determined by a direct search in the complex momentum plane and by using the inverse determinant method [14].

It is seen from the Table that all combinations of the two-body interactions lead to a quasi-bound state in the  $\bar{K}\bar{K}N$  three-body system. Thus, the repulsion in the  $\bar{K}\bar{K}$  subsystem is more than compensated by the attraction provided by the interaction in the  $\bar{K}N$  subsystem(s) and does not prevent the formation of a quasi-bound state.

Comparing the poles for  $\bar{K}\bar{K}N$ , obtained with the two-pole models of the  $\bar{K}N$  interaction, we see that the chirally motivated potential leads to a more shallow quasi-bound state

TABLE II. Pole positions (in MeV) of the quasi-bound state in the  $\bar{K}\bar{K}N$  system. Results of the direct pole search and of the inverse determinant method are given, employing various combinations of the  $\bar{K}\bar{K}$  and  $\bar{K}N$  in the AGS equations, see description in the text. Two-body pole position(s) of the  $\bar{K}N$  potentials are also presented. The two- and three-body thresholds are situated at 1434.57 and 1930.21 MeV, respectively.

		$\bar{K}\bar{K}N$ pole, direct search	$\bar{K}\bar{K}N$ pole, inverse determinant	$\bar{K}N$ pole(s)
$V_{\bar{K}\bar{K}}^{Orig}$	$V_{\bar{K}N-\pi\Sigma}^{1,SIDD}$	1918.31 - $i$ 51.14	1913.14 - $i$ 55.39	1428.14 - $i$ 46.81
	$V_{\bar{K}N-\pi\Sigma}^{2,SIDD}$	1907.15 - $i$ 45.69	1906.49 - $i$ 38.81	1418.11 - $i$ 57.01
				1382.03 - $i$ 104.15
	$V_{\bar{K}N-\pi\Sigma-\pi\Lambda}^{Chiral}$	1914.70 - $i$ 31.75	1914.34 - $i$ 28.71	1418.08 - $i$ 32.83
				1407.03 - $i$ 88.31
$V_{\bar{K}\bar{K}}^{Latt}$	$V_{\bar{K}N-\pi\Sigma}^{1,SIDD}$	1910.70 - $i$ 51.01	1906.51 - $i$ 51.85	1428.14 - $i$ 46.81
	$V_{\bar{K}N-\pi\Sigma}^{2,SIDD}$	1904.28 - $i$ 42.30	1903.81 - $i$ 38.39	1418.11 - $i$ 57.01
				1382.03 - $i$ 104.15
	$V_{\bar{K}N-\pi\Sigma-\pi\Lambda}^{Chiral}$	1914.12 - $i$ 30.66	1914.27 - $i$ 29.96	1418.08 - $i$ 32.83
				1407.03 - $i$ 88.31

than the phenomenological one. We believe that this must be connected with the energy dependence of the former potential, because the real parts of the higher two-body pole position corresponding to the  $\Lambda(1405)$  resonance are almost the same for the both potentials, see Table II (right column). Comparing the widths of the states we see that for the chirally motivated  $V_{\bar{K}N}^{Chiral}$  the width of the  $\bar{K}N$  state and that of the  $\bar{K}\bar{K}N$  state are almost the same. The phenomenological  $V_{\bar{K}N}^{2,SIDD}$  with a broader “ $\Lambda(1405)$ ” leads to a noticeably more narrow  $\bar{K}\bar{K}N$  state, which, however, is still wider than the “chirally motivated” one. The situation is opposite for the one-pole  $V_{\bar{K}N}^{1,SIDD}$  model, where the two-body quasi-bound  $\bar{K}N$  state is more narrow than the three-body  $\bar{K}\bar{K}N$  state. In this context we want to mention that a somewhat surprising behaviour of the results was also observed in [32] in the  $K^-d \rightarrow \pi\Sigma N$  spectra based on the  $V_{\bar{K}N}^{1,SIDD}$  potential – in contrast to the ones for other phenomenological  $\bar{K}N$  models. Since another one-pole potential used in [32] behaves quite normaly, it seems

that the different trend seen in the calculations with  $V_{\bar{K}N}^{1,SIDD}$  could be due to some peculiar features of this particular one-pole potential.

The results obtained with the phenomenological  $\bar{K}N$  potentials exhibit more sensitivity to the  $\bar{K}\bar{K}$  interaction than the chirally motivated interaction. As was expected, the less repulsive  $\bar{K}\bar{K}$  model that simulates the lattice QCD results leads to somewhat deeper quasi-bound three-body state than the  $\bar{K}\bar{K}$  interaction based on the original Jülich  $\pi\pi - \bar{K}K$  model. The largest difference between results based on the potentials  $V_{\bar{K}\bar{K}}^{Orig}$  and  $V_{\bar{K}\bar{K}}^{Latt}$  were obtained with the one-pole phenomenological  $V_{\bar{K}N}^{1,SIDD}$  model. A less repulsive  $\bar{K}\bar{K}$  interaction also leads to a more narrow  $\bar{K}\bar{K}N$  quasi-bound state in all the cases.

A comparison of the pole positions obtained from the direct pole search to the ones that follow from the inverse determinant method reveals that the accuracy of the second method is much lower for the phenomenological  $\bar{K}N$  interactions than for the chirally motivated one. This is an expected result keeping in mind the larger widths of the "phenomenological"  $\bar{K}\bar{K}N$  states. The one-to-one connection between a complex pole and the Breit-Wigner form of the corresponding bump on the real axis is obviously less pronounced if the pole is situated further away from the real axis.

It is also interesting to compare the binding energies and widths of the quasi-bound states in the  $\bar{K}\bar{K}N$  system with those for  $\bar{K}NN$ , obtained in [14]. In both three-body systems the strongly attractive  $\bar{K}N$  interaction is present and plays an essential role. We see that for a specific  $\bar{K}N$  potential the quasi-bound state in the strangeness  $S = -2$   $\bar{K}\bar{K}N$  system is only about half as deep as that in the  $S = -1$  three-body system. The  $\bar{K}\bar{K}N$  states are also much broader, especially those obtained with the phenomenological  $\bar{K}N$  models. The differences in the binding energies are expected since the  $NN$  interaction appearing in  $\bar{K}NN$  is attractive, while the  $\bar{K}\bar{K}$  interaction in  $\bar{K}\bar{K}N$  is repulsive. Their (attractive or repulsive) character is, probably, the origin of the differences in the widths too.

As already said in the Introduction, there has been a previous investigation on the  $\bar{K}\bar{K}N$  system [6]. Though the binding energies reported in that work are of the same order of magnitude we want to emphasize that in reality it is difficult to compare our results with the ones in that paper. The authors of [6] used energy-independent as well as energy-dependent potentials, but the two-body energy of the latter is fixed arbitrarily. Moreover, the imaginary parts of all complex potentials are completely ignored in their variational calculations. That imaginary parts are treated only perturbatively, which, probably, is one

of the reasons of the strong underestimation of the  $\bar{K}\bar{K}N$  widths in comparison to ours. In a series of works devoted to the  $\bar{K}NN$  system we demonstrated that a proper inclusion of the lower-lying channels – either by a direct inclusion or by using the exact optical potential, see e.g. [15, 21] – is very important. Therefore, the results of Ref. [6], involving several uncontrolled approximations, can be considered only as a very rough estimation.

## V. CONCLUSIONS

We presented a dynamically exact calculation of a quasi-bound state in the  $\bar{K}\bar{K}N$  three-body system, performed in the framework of Faddeev-type AGS equations. As input we used two phenomenological and one chirally motivated  $\bar{K}N$  potentials, which describe the experimental information on the  $\bar{K}N$  system equally well and produce either a one- or two-pole structure of the  $\Lambda(1405)$  resonance. For the  $\bar{K}\bar{K}$  subsystem we resort to an interaction that is adjusted to the  $KK$   $s$ -wave scattering length recently determined in lattice QCD simulations. In addition a phenomenological  $\bar{K}\bar{K}$  potential based on meson-exchange is employed, which is derived by SU(3) symmetry arguments from the Jülich  $\pi\pi - \bar{K}K$  coupled-channels model. The position and width of the  $\bar{K}\bar{K}N$  quasi-bound state were evaluated in two ways: (i) by a direct pole search in the complex energy plane and (ii) using the inverse determinant method.

We found that a quasi-bound state exists in the  $\bar{K}\bar{K}N$  system in spite of the repulsive character of the  $\bar{K}\bar{K}$  interaction. Its binding energy and width are in the region 12 – 26 MeV and 61 – 102 MeV, respectively, where the variation reflects the uncertainty due to differences in the two-body input. The quasi-bound state in the strangeness  $S = -2$   $\bar{K}\bar{K}N$  system turned out to be much shallower and broader than the one in the  $S = -1$   $\bar{K}NN$  system, when comparing calculations with the same  $\bar{K}N$  potential.

What are the perspectives of finding the  $\bar{K}\bar{K}N$  quasi-bound state in experiments? This state has the same quantum numbers as a  $\Xi$  baryon with  $J^P = (1/2)^+$ , as already noted in [6]. The available experimental information on the  $\Xi$  spectrum is rather limited, see [31], and for  $(1/2)^+$  only the ground state (with an isospin-averaged mass of 1318 MeV) is established. The quark model [33] predicts a first excited state at around 1700 MeV and another one around 1950 MeV, where the latter is already above the  $\bar{K}\bar{K}N$  threshold. There is a  $\Xi(1950)$  listed by the PDG but its quantum numbers  $J^P$  are not determined and it is

unclear whether it should be identified with the quark-model state. Indeed the PDG suggests that there could be even more than one resonance in this region because the mass values of the experimental evidence summarized in the listing [31] scatter over 70 MeV or so. It is interesting to see that four of the values would be roughly consistent with the quasi-bound state found in the present study. Specifically, the experiment reported in Ref. [34] yielded a mass of  $1894 \pm 18$  MeV and a width of  $98 \pm 23$  MeV that is more or less compatible with the range of values for the pole position that emerged from our three-body calculation. In any case, in view of concrete plans for experiments dedicated to  $\Xi$  baryon spectroscopy at J-PARC [35] and JLAB [36, 37] there are good chances that more information about the strangeness  $S = -2$  resonances will become available. Probably, then one can draw more solid conclusions on the  $\bar{K}\bar{K}N$  quasi-bound state.

**Acknowledgments.** The work was supported by the Czech CACR grant 15-04301S. One of the authors (NVS) is thankful to J. Révai for fruitful discussions.

- 
- [1] Y. Nogami, Phys. Lett. **7**, 288 (1963).
  - [2] T. Yamazaki and Y. Akaishi, Phys. Lett. B **535**, 70 (2002).
  - [3] N.V. Shevchenko, J. Révai, Phys. Rev. C **90**, 034003 (2014).
  - [4] R. W. Griffith, Phys. Rev. **176**, 1705 (1968).
  - [5] J. W. Chen, D. O’Connell and A. Walker-Loud, Phys. Rev. D **75**, 054501 (2007).
  - [6] Y. Kanada-En’yo and D. Jido, Phys. Rev. C **78**, 025212 (2008).
  - [7] J. A. Oller and U. G. Meissner, Phys. Lett. B **500** (2001) 263.
  - [8] J. Révai, N.V. Shevchenko, Phys. Rev. C **79**, 035202 (2009).
  - [9] N.V. Shevchenko, Phys. Rev. C **85**, 034001 (2012).
  - [10] K. Sasaki *et al.* [PACS-CS Collaboration], Phys. Rev. D **89**, 054502 (2014).
  - [11] S. R. Beane *et al.* [NPLQCD Collaboration], Phys. Rev. D **77**, 094507 (2008).
  - [12] D. Lohse, J. W. Durso, K. Holinde, and J. Speth, Nucl. Phys. A **516**, 513 (1990).
  - [13] G. Janssen, B.C. Pearce, K. Holinde, and J. Speth, Phys. Rev. D **52**, 2690 (1995).
  - [14] J. Révai, N.V. Shevchenko, Phys. Rev. C **90**, 034004 (2014).
  - [15] N.V. Shevchenko, A. Gal, J. Mareš, J. Révai, Phys. Rev. C **76**, 044004 (2007).

- [16] T. Sekihara, arXiv:1505.02849 [hep-ph].
- [17] A. Ramos, E. Oset and C. Bennhold, Phys. Rev. Lett. **89**, 252001 (2002).
- [18] D. Aston *et al.*, Nucl. Phys. B **296**, 493 (1988).
- [19] D. Linglin *et al.*, Nucl. Phys. B **57**, 64 (1973).
- [20] P. Estabrooks, R. K. Carnegie, A. D. Martin, W. M. Dunwoodie, T. A. Lasinski and D. W. G. S. Leith, Nucl. Phys. B **133**, 490 (1978).
- [21] N.V. Shevchenko, Phys. Rev. C **85**, 034001 (2012).
- [22] N.V. Shevchenko, Nucl. Phys. A **890-891**, 50 (2012).
- [23] M. Sakitt *et al.*, Phys. Rev. **139**, B719 (1965).
- [24] J.K. Kim, Phys. Rev. Lett. **14**, 29 (1965); Columbia University Report, Nevis, 149 (1966); Phys. Rev. Lett. **19**, 1074 (1967).
- [25] W. Kittel, G. Otter, and I. Wacek, Phys. Lett. **21**, 349 (1966).
- [26] J. Ciborowski *et al.*, J. Phys. G **8**, 13 (1982).
- [27] D. Evans *et al.*, J. Phys. G **9**, 885 (1983).
- [28] D.N. Tovee *et al.*, Nucl. Phys. B **33**, 493 (1971).
- [29] R.J. Nowak *et al.*, Nucl. Phys. B **139**, 61 (1978).
- [30] M. Bazzi *et al.* (SIDDHARTA Collaboration), Phys. Lett. B **704**, 113 (2011).
- [31] K.A. Olive *et al.* (Particle Data Group), Chin. Phys. C **38**, 090001 (2014).
- [32] J. Révai, Few Body Syst. **54**, 1865 (2013), Few Body Syst. **54**, 1877 (2013).
- [33] K. T. Chao, N. Isgur, and G. Karl, Phys. Rev. D **23**, 155 (1980).
- [34] P. M. Dauber, J. P. Berge, J. R. Hubbard, D. W. Merrill and R. A. Muller, Phys. Rev. **179**, 1262 (1969).
- [35] M. Naruki and K. Shiotori, Letter of Intent, J-PARC PAC-18, 2014,  
[http://j-parc.jp/researcher/Hadron/en/pac\\_1405/pdf/LoI\\_2014-4.pdf](http://j-parc.jp/researcher/Hadron/en/pac_1405/pdf/LoI_2014-4.pdf)
- [36] L. Guo *et al.*, Phys. Rev. C **76**, 025208 (2007).
- [37] M.J. Amarian *et al.*, Letter of Intent, Jefferson Lab PAC-43, 2015,  
[http://argus.phys.uregina.ca/glueX/DocDB/0027/002759/001/klong\\_LOI.pdf](http://argus.phys.uregina.ca/glueX/DocDB/0027/002759/001/klong_LOI.pdf)

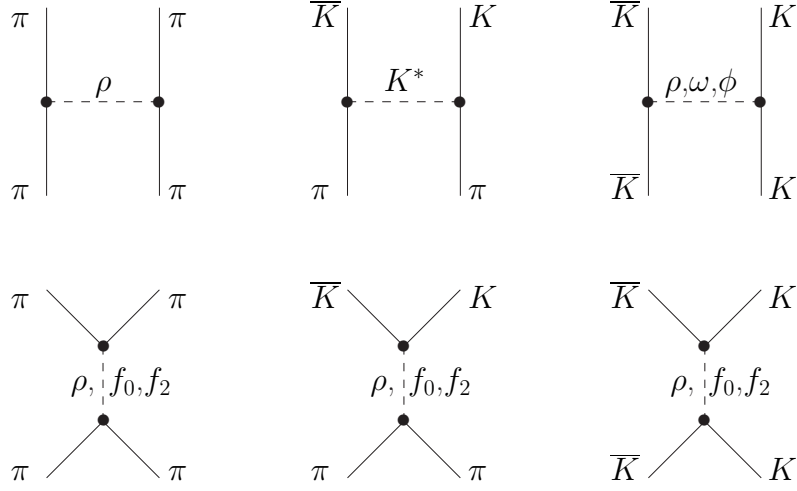


FIG. 1. Diagrams included in the Jülich  $\pi\pi - \bar{K}K$  potential [13].

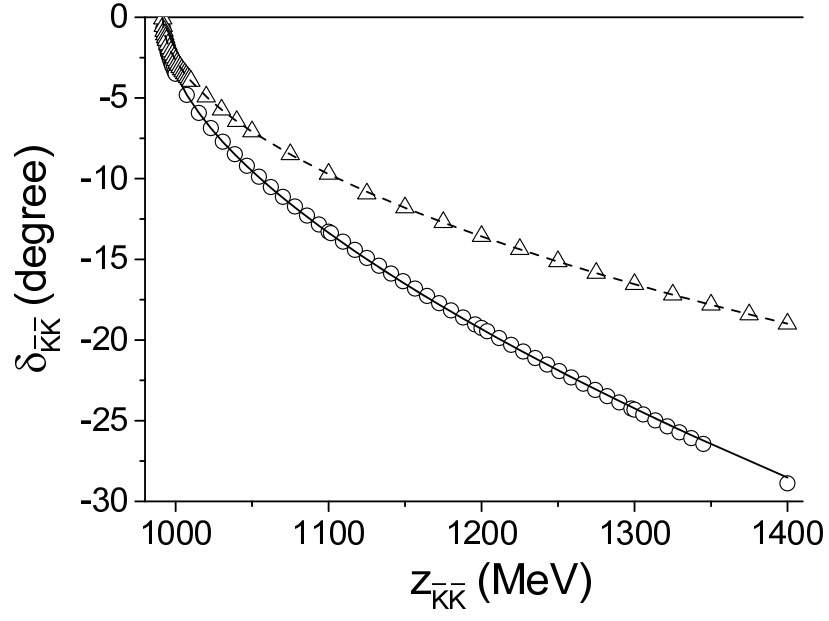


FIG. 2.  $\bar{K}\bar{K}$   $s$ -wave phase shifts in the  $I = 1$  state. The circles and the solid line denote the result of the “Original” Jülich model and its separable representation, respectively. The triangles and the dashed line are corresponding results for the “Lattice motivated”  $\bar{K}\bar{K}$  potentials.